

Liquid-Gas Phase Transitions and \mathcal{CK} Symmetry in Quantum Field Theories

Hirohichi Nishimura*

RIKEN BNL Research Center, Brookhaven National Laboratory, Upton NY 11973 USA

Michael C. Ogilvie[†] and Kamal Pangeni[‡]

Department of Physics, Washington University, St. Louis, MO 63130 USA

(Dated: 12/30/16)

A general field-theoretic framework for the treatment of liquid-gas phase transitions is developed. Starting from a fundamental four-dimensional field theory at nonzero temperature and density, an effective three-dimensional field theory with a sign problem is derived. Although charge conjugation \mathcal{C} is broken at finite density, there remains a symmetry under \mathcal{CK} , where \mathcal{K} is complex conjugation. We consider four models: relativistic fermions, nonrelativistic fermions, static fermions and classical particles. The thermodynamic behavior is extracted from \mathcal{CK} -symmetric complex saddle points of the effective field theory at tree level. The relativistic and static fermions show a liquid-gas transition, manifesting as a first-order line at low temperature and high density, terminated by a critical end point. In the cases of nonrelativistic fermions and classical particles, we find no first-order liquid-gas transitions at tree level. The mass matrix controlling the behavior of correlation functions is obtained from fluctuations around the saddle points. Due to the \mathcal{CK} symmetry of the models, the eigenvalues of the mass matrix can be complex. This leads to the existence of disorder lines, which mark the boundaries where the eigenvalues go from purely real to complex. The regions where the mass matrix eigenvalues are complex are associated with the critical line. In the case of static fermions, a powerful duality between particles and holes allows for the analytic determination of both the critical line and the disorder lines. Depending on the values of the parameters, either zero, one or two disorder lines are found. Numerical results for relativistic fermions give a very similar picture.

arXiv:1612.09575v1 [hep-th] 30 Dec 2016

* hnishimura@bnl.gov

† mco@physics.wustl.edu

‡ kamalpangeni@wustl.edu

I. INTRODUCTION

The problem of determining the phase structure of interacting particles at nonzero temperature and density is old and important. Modern field-theoretic approaches are typically susceptible to the sign problem, in which basic quantities such as the action becomes complex. This problem is particularly acute in the case of QCD at finite temperature and density: Lattice simulations have given excellent first-principles results for many observables of finite-temperature QCD, there has been less clear success when the chemical potential μ is nonzero [1–3]. A central problem is the determination of the phase structure of QCD at low temperature and density where a critical line with a critical end point in the Ising, or liquid-gas, universality class is widely expected.

Here we address the generic problem of liquid-gas phase transitions from a field theory perspective. The general class of field theories we will study is the class of \mathcal{CK} -symmetric models obtained from dimensional reduction of a four-dimensional field theory at finite temperature and density. The simplest case of interest are models with a single type of particles, interacting via a scalar field σ and a vector field A_μ . Both σ and A_μ will be taken to have masses. The potential induced by σ will be attractive, while that caused by the static vector potential A_4 will be repulsive between particles. The particles of the underlying theory are integrated out, and after dimensional reduction and redefinition of fields, we obtain a Lagrangian of the general form

$$L_{3d} = \frac{1}{2} (\nabla\phi_1)^2 + \frac{1}{2} m_1^2 \phi_1^2 + \frac{1}{2} (\nabla\phi_2)^2 + \frac{1}{2} m_2^2 \phi_2^2 - F(\phi_1, \phi_2) \quad (1)$$

where ϕ_1 is associated with the attractive force, and ϕ_2 with the repulsive force. The field ϕ_1 is naturally as a four-dimensional scalar, but ϕ_2 is obtained from the fourth component of a vector interaction. The function F can be interpreted as $\beta p(\phi_1, \phi_2)$, where β is the inverse of the temperature T and p is a local pressure. In particular, $p(\phi_1, \phi_2)$ is the local pressure of the gas of particles in the grand canonical ensemble in the presence of the background fields ϕ_1 and ϕ_2 .

The key feature of L_{3d} is that it is not real, but instead satisfies the \mathcal{CK} symmetry condition

$$L_{3d}(\phi_1, \phi_2)^* = L_{3d}(\phi_1, -\phi_2). \quad (2)$$

The \mathcal{C} transformation naturally takes $\phi_2 \rightarrow -\phi_2$ as in the case of QED, and the ϕ_1 field is left invariant. A nonzero chemical potential μ explicitly breaks \mathcal{C} symmetry, but the antilinear symmetry \mathcal{CK} remains [4–7]. \mathcal{CK} symmetry implies that the saddle points of L_{3d} have ϕ_2 purely imaginary; at these saddle points, L_{3d} is real. Analytic continuation of the fields into the complex plane leads to a resolution of the sign problem at tree level. More generally, unbroken \mathcal{CK} symmetry implies that the expected value of $\langle\phi_2\rangle$ must be zero or purely imaginary, because $\langle i\phi_2 \rangle^* = \langle i\phi_2 \rangle$.

The static solutions of the equations of motion take the form

$$m_1^2 \phi_1 = \frac{\partial F}{\partial \phi_1} \quad (3)$$

$$m_2^2 \phi_2 = \frac{\partial F}{\partial \phi_2}. \quad (4)$$

The presence of such a \mathcal{CK} symmetry is generic in quantum field theories at finite density. The mass matrix for ϕ_1 and ϕ_2 is given by

$$\begin{pmatrix} m_1^2 - \frac{\partial^2 F}{\partial \phi_1^2} & -\frac{\partial^2 F}{\partial \phi_1 \partial \phi_2} \\ -\frac{\partial^2 F}{\partial \phi_2 \partial \phi_1} & m_2^2 - \frac{\partial^2 F}{\partial \phi_2^2} \end{pmatrix}. \quad (5)$$

The mass matrix is nonhermitian because the off-diagonal elements are purely imaginary at the saddle point, where ϕ_2 is imaginary. It does, however, inherit the \mathcal{CK} symmetry of the underlying model. This in turn implies that the eigenvalues of the mass matrix are either both real or form a complex conjugate pair [4–7]. The boundary of the region where complex conjugate pairs occur is given by

$$\left(m_1^2 - \frac{\partial^2 F}{\partial \phi_1^2} - m_2^2 + \frac{\partial^2 F}{\partial \phi_2^2} \right)^2 + 4 \left(\frac{\partial^2 F}{\partial \phi_1 \partial \phi_2} \right)^2 = 0. \quad (6)$$

The occurrence of complex conjugate pairs of mass eigenvalues in turn lead to the damped sinusoidal density oscillations often associated with the presence of a liquid phase. Thus we see that this formalism can give a simple understanding of the existence of disorder lines, which mark a change in the behavior of the potential between particles from exponential to damped sinusoidal behavior. This behavior cannot be obtained from field theories with real actions.

One of the hallmarks of typical liquid-gas systems is the existence of regions in parameter space where density-density correlation functions exhibit damped oscillatory behavior. From the perspective of quantum field theory, the appearance of damped oscillatory behavior in correlation functions is unusual. Such behavior is prohibited in Euclidean quantum field theories with spectral positivity. The simplest model of the liquid-gas transition, the Ising model in its binary alloy form, has spectral positivity and cannot exhibit damped oscillatory behavior of its correlation functions. Damped oscillatory behavior occurs generally in the class of models we consider whenever a first-order critical line occurs.

We will consider four different models, corresponding to four different choices for the function $F(\phi_1, \phi_2)$. In the next section, we will consider the case of relativistic fermions of mass m , with F taken to be

$$F = \int \frac{d^3k}{(2\pi)^3} \log \left[1 + \exp \left(-\beta \sqrt{k^2 + (m - g\beta^{-1/2}\phi_1)^2} + \beta\mu + i\beta^{1/2}e\phi_2 \right) \right]. \quad (7)$$

The coupling constants g and e determine the strength of the attractive and repulsive forces respectively. There is a natural nonrelativistic limit, where after redefinition of the chemical potential we have

$$F = \int \frac{d^3k}{(2\pi)^3} \log \left[1 + \exp \left(-\beta k^2/2m + \beta\mu + \beta^{1/2}g\phi_1 + i\beta^{1/2}e\phi_2 \right) \right]. \quad (8)$$

Although the case of relativistic fermions exhibits a first-order liquid-gas transition, the nonrelativistic reduction does not. The third section considers the case of static fermions, where

$$F = \frac{1}{v} \log \left[1 + \exp \left(-\beta m + \beta\mu + \beta^{1/2}g\phi_1 + i\beta^{1/2}e\phi_2 \right) \right] \quad (9)$$

where v is a parameter with dimensions of volume. This model also has a first-order liquid gas transition. However, its low-density reduction, the classical gas with

$$F = \frac{1}{v} \exp \left(-\beta m + \beta\mu + \beta^{1/2}g\phi_1 + i\beta^{1/2}e\phi_2 \right) \quad (10)$$

does not have a first-order transition and does not have stable ground state. On the other hand, its partition function is exactly equivalent to that of a classical gas, as we show in an appendix. A final section gives our conclusions.

II. RELATIVISTIC FERMIONS

In this section, we study the liquid-gas phase transition in a model of relativistic fermions. We begin by showing how an effective three-dimensional field theory can be derived from a fundamental field theory. This approach is general and can be applied to other models as well, such as relativistic or nonrelativistic bosons.

A. Derivation from fundamental field theory

We consider a relativistic fermion interacting with a scalar field σ of mass m_σ and a vector field A_μ of mass m_A . These fields couple to the fermion with coupling g and e respectively. The Lagrangian for the fermionic part is

$$L_F = \bar{\psi} [i\gamma \cdot (\partial - ieA - \mu\hat{e}_4) - (m - g\sigma)] \psi \quad (11)$$

where m is the fermion mass. The bosonic part is given by

$$L_B = \frac{1}{2} (\partial\sigma)^2 + \frac{1}{2} m_\sigma^2 \sigma^2 + \frac{1}{4} F_{\mu\nu}^2 + \frac{1}{2} m_A^2 A_\mu^2. \quad (12)$$

This can be considered to be a QED version of the PNJL model, that is, a PNJL model where the gauge symmetry is $U(1)$. We set the boson masses m_σ and m_A to be constant, although in practical applications of the formalism they may be temperature dependent. Any expected value for the boson fields σ and A_μ (actually the associated Polyakov loop) are induced in this model by the effects of the fermions at finite temperature and density. That said, it is completely straightforward to include potential terms for σ and A_4 that can produce a more complicated phase structure. For example, a potential for σ could give rise to the analog of the chiral transition in NJL and PNJL models. In this model, however, the liquid-gas transition is driven solely by the interactions between the fermions.

The finite-temperature one-loop effective potential in the presence of constant fields σ and A_4 takes the form

$$S_{eff} = \int d^d x [V_\phi + V_A + V_{FT}] \quad (13)$$

where the temperature-dependent part of the one-loop fermionic contribution to the effective potential V_{FT} is given by

$$V_{FT} = -\frac{1}{\beta} \int \frac{d^3 k}{(2\pi)^3} \log \left[1 + \exp \left(-\beta \sqrt{k^2 + (m - g\sigma)^2} + \beta\mu + i\beta e A_4 \right) \right] \quad (14)$$

and V_σ and V_A are quadratic. Although there are also contributions from thermal excitations of σ and A_μ , we ignore them here because they do not affect the phase structure. For simplicity, we generally assume that μ is sufficiently large that the antiparticle contribution can be suppressed. However, in the case of relativistic fermions, antiparticle effects must be included to obtain the correct phase structure near $\mu = 0$, so in this case antiparticle effects are included. For comparison with the other models, we do not denote these effect explicitly here. The potential V_{FT} is nothing but the negative of the pressure of a relativistic fermion moving in the constant background provided by σ and A_4 . For slowly varying fields σ and A_μ , V_{FT} represents the lowest order fermionic contribution in a derivative expansion of the effective action [8]. We have also assumed that the spatial part of the vector field can be neglected, so that only the timelike component of A_μ need be included.

We dimensionally reduce to a three-dimensional effective theory, yielding an effective Lagrangian L_{3d} of the form

$$L_{3d} = \beta L_B + \beta V_{FT}.$$

We define new variables $\phi_1 = \beta^{1/2}\sigma$ and $\phi_2 = \beta^{1/2}A_4$ so as to maintain the canonical kinetic terms and also set $m_1 = m_\sigma$ and $m_2 = m_A$, giving

$$L_{3d} = \frac{1}{2} (\nabla\phi_1)^2 + \frac{1}{2} m_1^2 \phi_1^2 + \frac{1}{2} (\nabla\phi_2)^2 + \frac{1}{2} m_2^2 \phi_2^2 - \int \frac{d^3 k}{(2\pi)^3} \log \left[1 + \exp \left(-\beta \sqrt{k^2 + (m - g\beta^{-1/2}\phi_1)^2} + \beta\mu + i\beta^{1/2}e\phi_2 \right) \right]. \quad (15)$$

The last term in the expression is the definition of $F(\phi_1, \phi_2)$ for this model.

B. Phase structure and disorder lines

The phase structure of the model is obtained from the static solutions of the equations of motion:

$$m_1^2 \phi_1 = \frac{\partial F}{\partial \phi_1} \quad (16)$$

$$m_2^2 \phi_2 = \frac{\partial F}{\partial \phi_2} \quad (17)$$

while the presence of disorder lines is determined from the mass matrix

$$\begin{pmatrix} m_1^2 - \frac{\partial^2 F}{\partial \phi_1^2} & -\frac{\partial^2 F}{\partial \phi_1 \partial \phi_2} \\ -\frac{\partial^2 F}{\partial \phi_2 \partial \phi_1} & m_2^2 - \frac{\partial^2 F}{\partial \phi_2^2} \end{pmatrix}. \quad (18)$$

In addition to T and μ , all of the models we consider have five parameters: m , m_1 , m_2 , e and g . This is a very large parameter space to explore. In general, the potential takes the form $F(\phi_1, \phi_2) \rightarrow F(g\phi_1, e\phi_2)$. In terms of the rescaled fields $\tilde{\phi}_1 = g\phi_1$ and $\tilde{\phi}_2 = e\phi_2$, we can write the equation of motion as

$$\frac{1}{\kappa_1} \tilde{\phi}_1 = \frac{\partial F}{\partial \tilde{\phi}_1} \quad (19)$$

$$\frac{1}{\kappa_2} \tilde{\phi}_2 = \frac{\partial F}{\partial \tilde{\phi}_2} \quad (20)$$

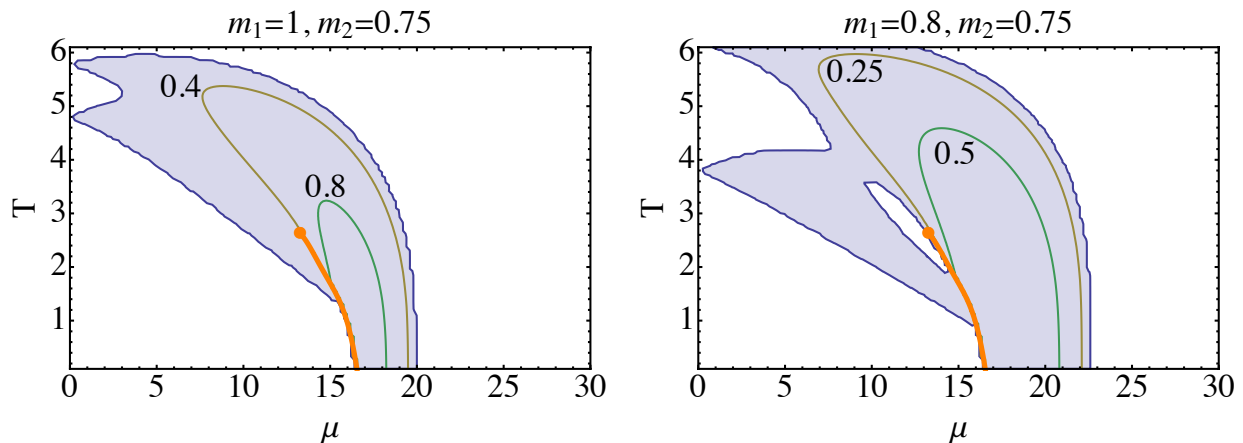


Figure 1. Phase diagrams for relativistic fermions for $m = 20$ and $m_2 = 0.75$ with $e = 0.3$. In the first graph $g_1 = m_1 = 1$, while in the second $g_1 = m_1 = 0.8$. The shaded region indicates where the mass matrix eigenvalues form complex conjugate pairs, and the contour lines refer to the imaginary parts of the mass matrix eigenvalues. The boundary of the shaded region defines the disorder line in the phase diagram. Note the appearance of a second disorder line inside the first in the second graph. The thick line shows a first-order line emerging from the $T = 0$ axis and terminating in a critical end point.

where $\kappa_1 = g^2/m_1^2$ and $\kappa_2 = e^2/m_2^2$. It is then clear that in addition to T and μ , only three parameters, κ_1 , κ_2 and m determine the solution as well as the location of the critical line if there is one. On the other hand, the equation for the disorder line becomes

$$\left[\left(\frac{1}{\kappa_1} - \frac{\partial^2 F}{\partial \tilde{\phi}_1^2} \right) - \frac{e^2}{g^2} \left(\frac{1}{\kappa_2} - \frac{\partial^2 F}{\partial \tilde{\phi}_2^2} \right) \right]^2 + 4 \frac{e^2}{g^2} \left(\frac{\partial^2 F}{\partial \tilde{\phi}_1 \partial \tilde{\phi}_2} \right)^2 = 0 \quad (21)$$

so the disorder line depends on the additional parameter of e/g . Because we are interested in conventional liquid gas transitions, we will choose the fermion mass m to be substantially heavier than the masses m_1 and m_2 . In all the models we consider, we set $m = 20$, $\kappa_1 = 1$, and $e = 0.3$, and we then vary the value of κ_2 to see the change of phase diagrams, as well as the value of $g = m_1$ to observe the difference in disorder lines.

Generally speaking, the liquid-gas transition will occur for low temperatures and $\mu \lesssim m$. The left-hand graph of Figure 1 shows the phase diagram for $m = 20$, $m_1 = 1$ and $m_2 = 0.75$. The couplings are given by $e = 0.3$ and $g = 1$. The shaded region indicates where the mass matrix eigenvalues form complex conjugate pairs, and the contour lines refer to the imaginary parts of the mass matrix eigenvalues. The boundary of the shaded region defines the disorder line in the phase diagram. The thick line shows a first-order line emerging from the $T = 0$ axis and terminating in a critical end point. The disorder line has a somewhat surprising shape; we will return to this point later. The graph on the right-hand side of the figure shows what happens if m_1 and g are decreased to 0.8. The phase structure is essentially unchanged, and the old disorder line has changed only slightly. However, a new disorder line boundary has opened up near the critical end point, inside the region where complex mass matrix eigenvalues were previously found.

In Figure 2, we show a second pair of phase diagrams. The graph on the left-hand side has $m_1 = g = 1$ and $m_2 = 0.5$. As before, $e = 0.3$ and $m = 20$. The end point of the critical line is at a lower value of T and slightly shifted to the right, but is otherwise similar to the previous graphs. However, when we examine the eigenvalues of the mass matrix, we see something new: the real part of conjugate pair of mass matrix eigenvalues becomes negative in a region near the critical end point. This is not necessarily unphysical behavior. The mass matrix is the matrix of squared masses, which are in general complex. A sufficiently large phase in the complex mass will lead to a squared mass eigenvalue with a negative real part. The boundary of this region is denoted in the figure by a dashed line. We have checked carefully for alternative possibilities and have concluded that this is likely to represent the correct phase structure of the model. We will return to this point in our conclusions after examining results from the other models. The graph on the right-hand side of the figure has $m_1 = g = 0.6$ and again has $m_2 = 0.5$, $e = 0.3$ and $m = 20$. The lower values of g and m_1 eliminate the region where the real part of the conjugate pair of mass matrix eigenvalues becomes negative. The shaded region becomes larger, but the values of the imaginary parts become smaller.

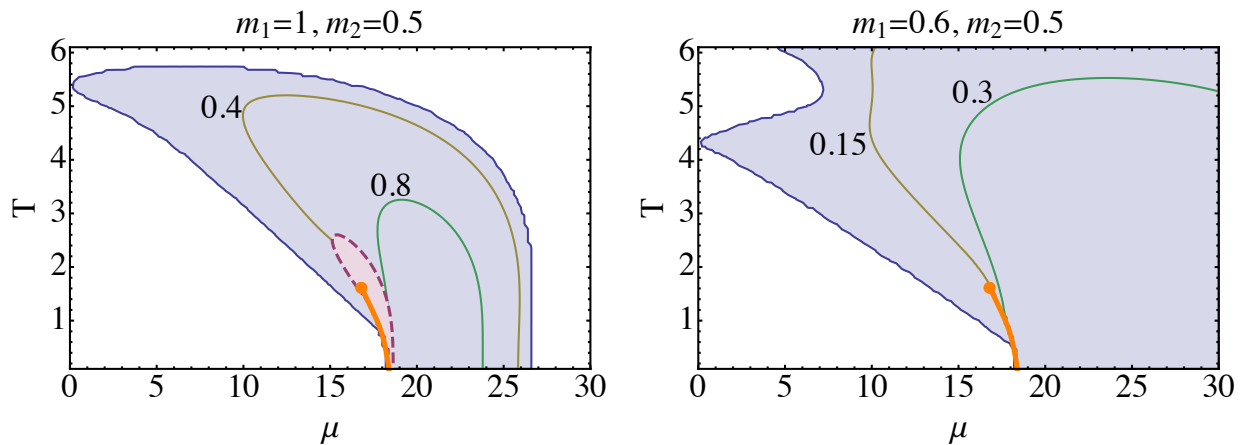


Figure 2. Phase diagrams for relativistic fermions for $m = 20$ and $m_2 = 0.5$ with $e = 0.3$. In the first graph $g_1 = m_1 = 1$, while in the second $g_1 = m_1 = 0.6$. The shaded region indicates where the mass matrix eigenvalues form complex conjugate pairs, and the contour lines refer to the imaginary parts of the mass matrix eigenvalues. The boundary of the shaded region defines the disorder line in the phase diagram. In the first graph, the dashed line near the critical end point is the boundary of the regions where the real parts of the mass matrix eigenvalues are negative. The thick line shows a first-order line emerging from the $T = 0$ axis and terminating in a critical end point.

C. Nonrelativistic Fermions

The case of nonrelativistic fermions can be obtained straightforwardly from the relativistic case, yielding the effective Lagrangian

$$L_{3d} = \frac{1}{2} (\nabla\phi_1)^2 + \frac{1}{2} m_1^2 \phi_1^2 + \frac{1}{2} (\nabla\phi_2)^2 + \frac{1}{2} m_2^2 \phi_2^2 - \int \frac{d^3k}{(2\pi)^3} \log \left[1 + \exp \left(-\beta k^2 / 2m + \beta\mu - \beta m + \beta^{1/2} g\phi_1 + i\beta^{1/2} e\phi_2 \right) \right]. \quad (22)$$

An important simplification occurs because the fields ϕ_1 and ϕ_2 appear in F only as the combination $\Phi = \beta^{1/2} g\phi_1 + i\beta^{1/2} e\phi_2$. The equations of motion for static solutions become

$$\phi_1 = \frac{\beta^{1/2} g}{m_1^2} \frac{\partial F}{\partial \Phi} \quad (23)$$

$$\phi_2 = i \frac{\beta^{1/2} e}{m_2^2} \frac{\partial F}{\partial \Phi}. \quad (24)$$

Combining these equations, we obtain

$$\Phi = \left(\frac{\beta g^2}{m_1^2} - \frac{\beta e^2}{m_2^2} \right) \frac{\partial F}{\partial \Phi}. \quad (25)$$

Defining

$$\kappa = \kappa_1 - \kappa_2 = \frac{g^2}{m_1^2} - \frac{e^2}{m_2^2} \quad (26)$$

we see that the phase diagram is determined by the single equation

$$\Phi = \beta \kappa \frac{\partial F}{\partial \Phi} \quad (27)$$

with the four parameters m_1 , m_2 , e and g collapsing into a single parameter κ . The solutions of this equation are extrema of the synthetic potential

$$U = \frac{1}{2} \Phi^2 - \beta \kappa F(\Phi). \quad (28)$$

This simplification also holds for static and classical particles as well.

Unlike the case of relativistic fermions, we find no liquid-gas transition in the case of nonrelativistic fermions. This can be very simply from the behavior of the potential U , which always has a single minimum.

III. STATIC FERMIONS

In this section, we study the behavior of static continuum fermions, which have no kinetic energy. The potential is given by

$$V_{static} = -\frac{1}{\beta v} \log [1 + \exp(-\beta m + \beta g \sigma + \beta \mu + i \beta e A_4)] \quad (29)$$

where v should be thought of as some volume associated with the particle. For lattice models, this is a natural limit at nonzero temperature where very heavy particles are fixed on a spatial lattice site. For continuum field theories, there is no systematic approximation which yields static fermions as a natural limit. Aside from the connection with lattice gauge theory, there are nevertheless good reasons to consider this model. The lattice form of this model was studied by Park and Fisher as a tool for demonstrating that the repulsive-core phase transition at negative $z \equiv \exp \beta (\mu - m)$ is in the $i\phi^3$ universality class [9]. The continuum model plays a similar role, illustrating both a liquid-gas transition in the usual Ising universality class and a repulsive-core transition in the $i\phi^3$ universality class for $z < 0$. The model is also interesting because it has an exact particle-hole symmetry that allows us to determine analytically the location of the critical line as well as some of the other key features of the model. This model reduces to the classical model in the limit where $z \exp \Phi \ll 1$. In that case the parameter v can be identified as $\lambda_T^3 = (2\pi/mT)^{3/2}$, but that identification is special to the low-density limit.

The dimensionally reduced effective Lagrangian L_{3d} has the form

$$L_{3d} = \frac{1}{2} (\nabla \phi_1)^2 + \frac{1}{2} m_1^2 \phi_1^2 + \frac{1}{2} (\nabla \phi_2)^2 + \frac{1}{2} m_2^2 \phi_2^2 - \frac{1}{v} \log \left[1 + \exp \left(-\beta m + \beta^{1/2} g \phi_1 + \beta \mu + i \beta^{1/2} e \phi_2 \right) \right]. \quad (30)$$

As was the case with nonrelativistic fermions, the crucial simplifying feature of this model, is that F depends on ϕ_1 and ϕ_2 only through $\Phi = \beta^{1/2} g \phi_1 + i \beta^{1/2} e \phi_2$. The static equations of motion reduce to

$$\Phi = \beta \kappa \frac{\partial F}{\partial \Phi} \quad (31)$$

which in this case can be written as

$$\Phi = \left(\frac{\beta \kappa}{v} \right) \frac{\partial}{\partial \Phi} \log [1 + z \exp(\Phi)]. \quad (32)$$

The corresponding potential U takes the form

$$U = \frac{1}{2} \Phi^2 - \kappa y \log [1 + z \exp(\Phi)] \quad (33)$$

where we have introduced for convenience $y = \beta/v$.

This model has a conventional liquid-gas transition for $\kappa y > 0$ and $z > 0$. We can locate the critical point of this model analytically. The second derivative of the potential $d^2U/d\Phi^2$ has two inflection points when $\kappa y > 4$; hence the potential U itself has two minima for $\kappa y > 4$. At the critical end point, the minimum of the potential coalesces with the two inflection points and one finds the critical end point at ($\kappa y = 4, z = e^{-2}$). Note that for $\kappa < 0$, there is a phase transition for $z < 0$; this transition is in the $i\phi^3$ universality class as discussed by Park and Fisher[9]. As they show, the phase structure may also be understood graphically. The equation $\partial U/\partial \Phi = 0$ may easily be written in the form

$$\Phi \exp(-\Phi) = \kappa y z - z \Phi \quad (34)$$

and the solutions found from the intersection of the left- and right-hand sides.

A. Particle-Hole Duality

Analytic information about the phase structure may be obtained from an exact duality argument [7] that exchanges particle and holes. We can rewrite U as

$$U = \frac{1}{2}\Phi^2 - \kappa y \log [1 + z^{-1}e^{-\Phi}] - \kappa y \Phi - \kappa y \log z \quad (35)$$

or

$$U = \frac{1}{2}(\Phi - \kappa y)^2 - \kappa y \log [1 + z^{-1}e^{-\Phi}] - \kappa y \log z - \frac{1}{2}(\kappa y)^2. \quad (36)$$

After shifting $\Phi \rightarrow \Phi' = -\Phi + \kappa y$, we have

$$U = \frac{1}{2}\Phi'^2 - \kappa y \log [1 + z^{-1}e^{\Phi' - \kappa y}] - \kappa y \log z - \frac{1}{2}(\kappa y)^2 \quad (37)$$

so the phase structure as revealed by Φ is invariant under

$$z \rightarrow z' = z^{-1}e^{-\kappa y} \quad (38)$$

$$\Phi \rightarrow \Phi' = -\Phi + \kappa y \quad (39)$$

These results can be extended to the potential V , where the duality transformation acts on ϕ_1 and ϕ_2 as

$$\phi_1 \rightarrow \phi'_1 = -\phi_1 + \frac{\beta^{1/2}g}{vm_1^2} \quad (40)$$

$$\phi_2 \rightarrow \phi'_2 = -\phi_2 + \frac{i\beta^{1/2}e}{vm_2^2} \quad (41)$$

consistent with the duality transformation of Φ .

The critical line must map into itself under this transformation and thus must form part of the curve

$$z = e^{-\kappa y/2}. \quad (42)$$

This is

$$\mu = m - \frac{\kappa}{2v} = m - \frac{1}{2v} \left(\frac{g^2}{m_1^2} - \frac{e^2}{m_2^2} \right). \quad (43)$$

The critical end point at $(\kappa y = 4, z = e^{-2})$ lies on the critical line and maps onto itself under duality. In more physical units, we have for the critical end point $T_{cep} = \kappa/4v$ and $\mu_{cep} = m - 2T_{cep}$. Along the critical line, the jump in Φ is given by

$$\Delta\Phi = \Phi - \Phi' = 2\Phi - \kappa y. \quad (44)$$

This is zero at the critical end point, which must occur when $\Phi = \kappa y/2$, consistent with the location of the critical end point.

The disorder lines associated with the mass matrix

$$\begin{pmatrix} m_1^2 - \frac{\partial^2 F}{\partial \phi_1^2} & -\frac{\partial^2 F}{\partial \phi_1 \partial \phi_2} \\ -\frac{\partial^2 F}{\partial \phi_2 \partial \phi_1} & m_2^2 - \frac{\partial^2 F}{\partial \phi_2^2} \end{pmatrix} \quad (45)$$

occur when the two eigenvalues are degenerate. Using the fact is a function of Φ , we arrive after some algebra at the condition

$$m_1^2 - m_2^2 - \beta (g \pm e)^2 \frac{\partial^2 F}{\partial \Phi^2} = 0. \quad (46)$$

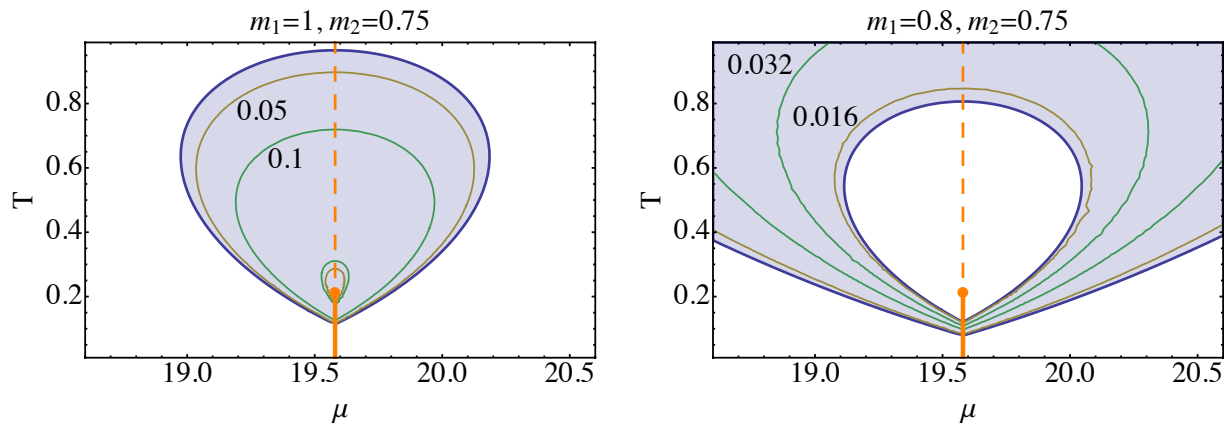


Figure 3. Phase diagrams for static fermions for $m = 20$ and $m_2 = 0.75$ with $e = 0.3$. In the first graph $g_1 = m_1 = 1$, while in the second $g_1 = m_1 = 0.8$. The shaded region indicates where the mass matrix eigenvalues form complex conjugate pairs, and the contour lines refer to the imaginary parts of the mass matrix eigenvalues. The boundary of the shaded region defines the disorder line in the phase diagram. Note the appearance of a second disorder line inside the first in the second graph. The thick line shows a first-order line emerging from the $T = 0$ axis and terminating in a critical end point. The dashed vertical line emerging from the critical end point is the line of particle-hole duality.

This equation for the disorder lines holds whenever F is a function only of Φ rather than ϕ_1 and ϕ_2 separately; this includes the cases of the nonrelativistic fermionic gas and the classical gas as well as the case of static fermions. For static fermions, this equation may be written as

$$m_1^2 - m_2^2 - \beta (g \pm e)^2 \frac{1}{v} \frac{z \exp \Phi}{(1 + z \exp \Phi)^2} = 0. \quad (47)$$

Because the first term in the sum is always positive and the second and third terms are always negative, we must have $m_1 \geq m_2$ for disorder lines to appear. The appearance of a factor $(g \pm e)^2$ in the third term makes possible the appearance of two distinct disorder lines, defining two distinct boundaries for the region where the mass matrix eigenvalues have imaginary parts. The negative contribution of the third term is larger in magnitude for the combination $g + e$; this indicates that it is possible to have zero, one or two disorder lines.

B. Phase structure and disorder lines

As we did in the case of relativistic fermions, we will choose the fermion mass m to be substantially heavier than the masses m_1 and m_2 , with $m = 20$. The left-hand graph of Figure 3 shows the phase diagram for $m = 20$, $m_1 = 1$ and $m_2 = 0.75$. The couplings are given by $e = 0.3$ and $g = 1$. These are exactly the same values as those used for the first graph in Figure 1. We set $v = 1$ throughout. The vertical line is the line of particle-hole self-duality; the lower portion of this line is a line of first-order phase transitions, terminated by a critical end point. The shaded region again indicates where the mass matrix eigenvalues form complex conjugate pairs, and the contour lines refer to the imaginary parts of the mass matrix eigenvalues. The reflection symmetry of the diagram about the self-dual line is due to particle-hole duality. With these parameters, we see that there is a single disorder line. The graph on the right-hand side of the figure shows what happens if m_1 and g are decreased to 0.8 while m_2 is set to 0.75. As was the case with relativistic fermions, the phase structure is essentially unchanged, but a new disorder line boundary has opened up around the critical end point, inside the region where complex mass matrix eigenvalues were previously found.

In Figure 4, we show a second pair of phase diagrams. The graph on the left-hand side has $m_1 = g = 1$ and $m_2 = 0.35$. As was the case with relativistic fermions, we find a small region around the critical end point where real parts of the eigenvalues of the mass matrix become negative. The boundary of this region is again denoted by a dashed line. The graph on the right-hand side of the figure has $m_1 = g = 0.4$ and $m_2 = 0.35$. The lower values of g and m_1 again eliminate the region where the real part of the conjugate pair of mass matrix eigenvalues becomes negative. The shaded region becomes larger, but the values of the imaginary parts become smaller. This behavior is again similar to what we found for relativistic fermions.

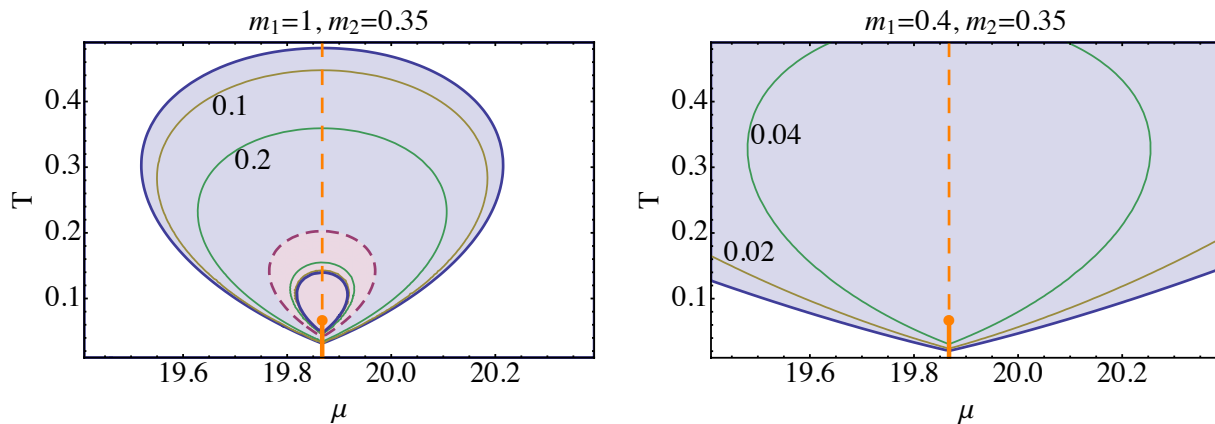


Figure 4. Phase diagrams for static fermions for $m = 20$ and $m_2 = 0.35$ with $e = 0.3$. In the first graph $g_1 = m_1 = 1$, while in the second $g_1 = m_1 = 0.4$. The shaded region indicates where the mass matrix eigenvalues form complex conjugate pairs, and the contour lines refer to the imaginary parts of the mass matrix eigenvalues. The boundary of the shaded region defines the disorder line in the phase diagram. In the first graph, the dashed line near the critical end point is the boundary of the regions where the real parts of the mass matrix eigenvalues are negative. The thick line shows a first-order line emerging from the $T = 0$ axis and terminating in a critical end point. The dashed vertical line emerging from the critical end point is the line of particle-hole duality.

C. Classical Particles

It is easy to obtain the effective field theory associated with the classical gas as a limit of the static fermion case. As mentioned previously, the correct behavior is obtained when $z \exp \Phi \ll 1$. The potential U can be written as

$$U = \frac{1}{2}\Phi^2 - \kappa y z \exp(\Phi). \quad (48)$$

The equation $\partial U / \partial \Phi = 0$ now becomes

$$\Phi \exp(-\Phi) = \kappa y z. \quad (49)$$

This equation is solved by the Lambert function W : $\Phi = -W(-\kappa y z)$. More intuitively, it may be solved graphically by plotting $\Phi e^{-\Phi}$, which must be $\kappa y z$. It is easy to see that there is no real solution for $\kappa y z > e^{-1}$, two solutions for $0 < \kappa y z < e^{-1}$ and one solution for $\kappa y z < 0$. Nowhere do we obtain the three solutions that would be expected with a standard first-order phase transition: two local minima separated by a local maximum. We can also visualize this result by noting that U is unbounded from below for $\kappa y z > 0$, with a local maximum and local minimum when $0 < \kappa y z < e^{-1}$, and no extrema for $\kappa y z > e^{-1}$. When $\kappa y z = e^{-1}$, there is a single static solution at $\Phi = 1$. It is easy to confirm that the mass matrix has a zero eigenvalue at this point, but it is not a conventional critical point; because it is unstable at cubic order, it is more like a spinodal point, where a metastable solution becomes unstable. It has been known for some time that a straightforward application of mean field theory to the classical liquid-gas system is insufficient to recover the critical behavior [10, 11]; it is therefore perhaps unsurprising that tree-level in an equivalent field theoretic approach is also insufficient.

IV. CONCLUSIONS

We have developed a framework for deriving and analyzing field-theoretic models of liquid-gas transitions and applied the formalism to some important models. In this framework, it is necessary to have two or more fields to include the effects of both attractive and repulsive potentials. The presence of a repulsive potential at nonzero μ gives rise to a sign problem in this class of field theories. Although charge conjugation symmetry is explicitly broken when $\mu \neq 0$, the symmetry \mathcal{CK} is unbroken, with profound consequences. One consequence of the \mathcal{CK} symmetry is that there are regions of the phase diagram where masses have imaginary parts, giving rise to damped oscillatory behavior in correlation functions. The border of these regions are disorder lines. This behavior cannot occur in conventional field theories without sign problems, as a consequence of spectral positivity.

We have found two models, relativistic fermions and static fermions, that have conventional liquid-gas transitions at tree level. In contrast, the field theories associated with nonrelativistic fermions and classical particles do not

have liquid-gas transitions at tree level. The case of static fermions has proven to be very tractable due to the exact particle-hole duality found there. As in our previous work on PNJL-type models of QCD [5, 6], the critical line of the liquid-gas transition is generally found in the phase diagram near any disorder lines present, although there does not seem to be any simple universal rule. The occurrence of zero, one or two disorder lines is easy to understand analytically in this model. In hindsight, the phase structure of relativistic fermions is qualitatively quite similar to that of static fermions. The absence of an exact particle-hole symmetry leads to a distortion of the features found in phase diagrams, but the overall behavior appears to be the same. Both models exhibit eigenvalues of the mass matrix with negative real parts for some regions of parameter space. Because the static fermion case is tractable, we believe that this behavior is physical, indicating regions where the phase of complex masses becomes sufficiently large. There are, however, other possibilities. It is possible that the incorrect solution is being used, or that the tree level approach fails when this occurs. Another possibility, discussed below, is that we have found regions where no equilibrium thermodynamic system exists. It is striking that the case of relativistic and static fermions have liquid-gas phase transitions at tree level, while nonrelativistic fermions and classical particles do not. It is not clear if this reflects some fundamental feature of the physical systems being modeled, or some limitation of the method used.

Many systems can be studied within the framework we have developed. However, we are acutely aware that not much is known about the stability of most of these systems. Sufficient conditions for the thermodynamic stability of systems of classical particles were developed some time ago by Fisher and Ruelle [12]. For example, the following conditions on the total potential $V = V_2 - V_1$ are sufficient for stability of a d -dimensional system: for some positive values of a_1 and a_2 , we have

$$r < a_1 V(r) \geq C/r^{d+\epsilon} \quad (50)$$

$$a_1 < r < a_2 V(r) \geq -w \quad (51)$$

$$r > a_2 V(r) \geq -C'/r^{d+\epsilon'} \quad (52)$$

where C , C' , w , ϵ and ϵ' are positive constants. A system with attractive and repulsive Yukawa potentials will satisfy these conditions if $e > g$. To our knowledge, there are no similar rigorous results for other systems. On physical grounds, we expect that fermionic systems will be stable whenever the corresponding classical system is stable. Because many of the current approaches to the sign problem, including the one used here, rely on saddle points in the complex plane of unknown stability, it would be very helpful to know for which parameter values a given system is thermodynamically stable.

APPENDIX

In the common case where F can be written as a function of $\Phi = \beta^{1/2}g\phi_1 + i\beta^{1/2}e\phi_2$, there is a formal equivalence between the partition function of the effective field theory and a generalized Liouville sine-Gordon field theory. This equivalence is a generalization of the equivalence of the sine-Gordon model with a Coulomb gas [13, 14]. The equivalence is proven by expanding $F(\Phi)$ in the action in a power series in z and integrating the resulting functional integrals exactly at each order in the expansion.

$$L_{3d} = \frac{1}{2}(\nabla\phi_1)^2 + \frac{1}{2}m_1^2\phi_1^2 + \frac{1}{2}(\nabla\phi_2)^2 + \frac{1}{2}m_2^2\phi_2^2 - F(\Phi). \quad (53)$$

The function F has a natural expansion of the form

$$F = \sum_n f_n e^{n\Phi}. \quad (54)$$

Expansion in the f_n leads to the interpretation of the partition function as the grand canonical partition function as a gas with multiple charges n and fugacities f_n ; some of the fugacities may be negative.

For simplicity, consider the case where only the $n = 1$ term is nonzero. Writing

$$F = \frac{z}{\lambda_T^d} e^{\Phi} \quad (55)$$

we can expand the partition function in powers of z :

$$Z = \int [d\phi] e^{-S_0} \sum_{k=0}^{\infty} \frac{1}{k!} \left(\frac{z}{\lambda_T^d} \right)^k \int d^d x_1 \dots d^d x_k \exp \left[\sum_{j=1}^k \Phi(x_j) \right] \quad (56)$$

where

$$S_0 = \int d^d x \left[\frac{1}{2} (\nabla \phi_1)^2 + \frac{1}{2} m_1^2 \phi_1^2 + \frac{1}{2} (\nabla \phi_2)^2 + \frac{1}{2} m_2^2 \phi_2^2 \right]. \quad (57)$$

Interchanging functional integration and summation and performing the Gaussian functional integrals we have

$$Z = \sum_{k=0}^{\infty} \frac{1}{k!} \left(\frac{z}{\lambda_T^d} \right)^k \int d^d x_1 \dots d^d x_k \exp \left\{ -\beta \sum_{k<l} [V_2(x_k - x_l) - V_1(x_k - x_l)] \right\} \quad (58)$$

where the Yukawa (screened Coulomb) potentials are determined by their Fourier transforms

$$\tilde{V}_1(q) = \frac{g_1^2}{q^2 + m_1^2} \quad (59)$$

$$\tilde{V}_2(q) = \frac{g_2^2}{q^2 + m_2^2} \quad (60)$$

The presence of terms in the expansion of F with $n = 1$ correspond to higher charges in the generalized Coulomb gas representation.

- [1] Philippe de Forcrand. Simulating QCD at finite density. *PoS*, LAT2009:010, 2009.
- [2] Sourendu Gupta. QCD at finite density. *PoS*, LATTICE2010:007, 2010.
- [3] Gert Aarts. Complex Langevin dynamics and other approaches at finite chemical potential. *PoS*, LATTICE2012:017, 2012.
- [4] Peter N. Meisinger and Michael C. Ogilvie. PT Symmetry in Classical and Quantum Statistical Mechanics. *Phil.Trans.Roy.Soc.Lond.*, A371:20120058, 2013. doi:10.1098/rsta.2012.0058.
- [5] Hiromichi Nishimura, Michael C. Ogilvie, and Kamal Pangaeni. Complex saddle points in QCD at finite temperature and density. *Phys. Rev.*, D90(4):045039, 2014. doi:10.1103/PhysRevD.90.045039.
- [6] Hiromichi Nishimura, Michael C. Ogilvie, and Kamal Pangaeni. Complex Saddle Points and Disorder Lines in QCD at finite temperature and density. *Phys. Rev.*, D91(5):054004, 2015. doi:10.1103/PhysRevD.91.054004.
- [7] Hiromichi Nishimura, Michael C. Ogilvie, and Kamal Pangaeni. Complex spectrum of finite-density lattice QCD with static quarks at strong coupling. *Phys. Rev.*, D93(9):094501, 2016. doi:10.1103/PhysRevD.93.094501.
- [8] Sidney R. Coleman and Erick J. Weinberg. Radiative Corrections as the Origin of Spontaneous Symmetry Breaking. *Phys. Rev.*, D7:1888–1910, 1973. doi:10.1103/PhysRevD.7.1888.
- [9] Youngah Park and Michael E. Fisher. Identity of the universal repulsive-core singularity with yang-lee edge criticality. *Phys. Rev. E*, 60:6323–6328, Dec 1999. doi:10.1103/PhysRevE.60.6323. URL <http://link.aps.org/doi/10.1103/PhysRevE.60.6323>.
- [10] J. Hubbard and P. Schofield. Wilson theory of a liquid-vapour critical point. *Physics Letters A*, 40(3):245 – 246, 1972. ISSN 0375-9601. doi:[http://dx.doi.org/10.1016/0375-9601\(72\)90675-5](http://dx.doi.org/10.1016/0375-9601(72)90675-5). URL <http://www.sciencedirect.com/science/article/pii/0375960172906755>.
- [11] Nikolai V. Brilliantov. Effective magnetic hamiltonian and ginzburg criterion for fluids. *Phys. Rev. E*, 58:2628–2631, Aug 1998. doi:10.1103/PhysRevE.58.2628. URL <http://link.aps.org/doi/10.1103/PhysRevE.58.2628>.
- [12] Michael E. Fisher and David Ruelle. The stability of many particle systems. *Journal of Mathematical Physics*, 7(2): 260–270, 1966. doi:10.1063/1.1704928. URL <http://dx.doi.org/10.1063/1.1704928>.
- [13] S. F. Edwards and A. Lenard. Exact statistical mechanics of a one dimensional system with coulomb forces. ii. the method of functional integration. *Journal of Mathematical Physics*, 3(4):778–792, 1962. doi:10.1063/1.1724281. URL <http://dx.doi.org/10.1063/1.1724281>.
- [14] Sidney R. Coleman. The Quantum Sine-Gordon Equation as the Massive Thirring Model. *Phys. Rev.*, D11:2088, 1975. doi:10.1103/PhysRevD.11.2088.